Differential Expression of Perforin in Muscle-infiltrating T Cells in Polymyositis and Dermatomyositis

Norbert Goebels,*‡ Dorothea Michaelis,* Martin Engelhardt,*§ Susanne Huber,* Anke Bender,* Dieter Pongratz,§ Margaret A. Johnson,‖ Hartmut Wekerle,* Jürg Tschopp,¶ Dieter Jenne,* and Reinhard Hohlfeld*‡

**Department of Neuroimmunology, Max-Planck-Institute of Psychiatry; D-82152 Martinsried, Germany, ‡Department of Neurology, Klinikum Grosshadern, D-81366 Munich, Germany; §Friedrich-Baur Institute, D-80336 Munich, Germany; ‖Muscular Dystrophy Group Research Laboratories, Newcastle General Hospital, Newcastle upon Tyne NE4 6BE, United Kingdom; and ¶Institute of Biochemistry, University of Lausanne, CH-1066 Epalinges, Switzerland*

Abstract

Polymyositis (PM) and dermatomyositis (DM) are the prototypical inflammatory diseases of skeletal muscle. In PM, CD8+ T cells invade and destroy muscle fibers, whereas humoral effector mechanisms prevail in DM. We studied the expression of the cytotoxic mediator perforin in inflammatory cells in PM and DM muscle by semiquantitative PCR, immunohistochemistry and confocal laser microscopy. Similar levels of perforin mRNA were expressed in PM and DM, and abundant perforin-expressing CD3+CD8+ and CD3+ CD4+ T cells were observed in both diseases. However, there was a striking difference in the intracellular localization of perforin. In DM, perforin was distributed randomly in the cytoplasm of the inflammatory T cells. In contrast, 43% of the CD8+ T cells that contacted a muscle fiber in PM showed perforin located vectorially towards the target muscle fiber. The results suggest (*a*) that the random distribution of perforin in the cytoplasm of muscle-infiltrating T cells observed in DM reflects nonspecific activation, and (*b*) that the vectorial orientation observed only in PM reflects the specific recognition via the T cell receptor of an antigen on the muscle fiber surface, pointing to a perforin- and secretion-dependent mechanism of muscle fiber injury. (*J. Clin. Invest.* 1996. 97:2905–2910.) Key words: autoimmune disease • myopathy • T cell • inflammation • cytotoxicity

Introduction

Perforin is an important membrane-damaging molecule of cell-mediated cytotoxic reactions in vitro (1–6). However, little is known about its role in human immunopathological conditions. In the present study, we have combined semiquantitative PCR and double-fluorescence immunohistochemistry to investigate the expression of perforin in two typical inflammatory disorders of skeletal muscle, polymyositis (PM)[1] and dermatomyositis (DM). Both in PM and DM, muscle contains mixed infiltrates of mononuclear cells (7–9). However, the immunological mechanisms of tissue injury are strikingly different. In PM, clonally expanded autoaggressive CD8+ T cells contact and invade muscle fibers (7, 10). This unique lesion allows morphological distinction between autoaggressive CD8+ T cells, bystander T cells, and target muscle fibers (7–9). In contrast to PM, humoral effector mechanisms prevail in DM (7–9). One of the earliest changes in DM is the focal depletion of muscle capillaries (11). Furthermore, immunofluorescence studies directly demonstrate the deposition of C5b-9 complement membrane attack complex in the microvascular endothelium in DM muscle, whereas morphological evidence for a cell-mediated attack against muscle fibers is absent (7–9). Therefore, PM and DM should serve as useful paradigms to study and compare the differential expression of perforin in lymphocyte subsets in situ. Our results show that in both diseases there is abundant expression of perforin in inflammatory T cells. However, only in PM is the perforin oriented vectorially towards the target muscle fiber, suggesting that the T cells recognize an (unknown) antigen on the muscle fiber and that perforin- and secretion-dependent mechanisms are involved in muscle fiber injury.

Methods

Clinical material. Diagnostic muscle biopsy specimens were obtained from five patients with PM and four (3 juvenile, 1 adult) patients with DM (8, 9). Four muscle specimens without myopathic changes (normal or neurogenic atrophy) served as controls. As controls for PCR studies, we used the human rhabdomysosarcoma cell line TE671 (ATCC, Rockville, MD), normal human myoblasts, CD8+ T cells and lymphokine-activated killer (LAK) cells. Normal human myoblasts were isolated and cultured according to standard methods as previously described (12). CD8+ T cells were isolated to > 90% purity from normal PBMC with anti-CD8 mAb (OKT8; ATCC) and anti–mouse IgG-coated magnetic beads (Stefan Miltenyi Biotech,

Address correspondence to Dr. Reinhard Hohlfeld, Department of Neuroimmunology, Max-Planck-Institute of Psychiatry, D-82152 Martinsried, Germany. Phone: 89-7095-4780; FAX: 89-7095-4782.

Received for publication 28 November 1995 and accepted in revised form 22 March 1996.

J. Clin. Invest.

0021-9738/96/06/2905/06 $2.00
Volume 97, Number 12, June 1996, 2905–2910

1. *Abbreviations used in this paper:* DM, dermatomyositis; LAK cells, lymphokine-activated killer cells; PM, polymyositis.

Bergisch Gladbach, Germany). LAK cells were generated from normal PBMC by stimulation with 5 μg/ml PHA (Wellcome, Dartford, UK) for 48 h.

Immunohistology. 7-μm cryostat sections of muscle were used for paired immunofluorescence studies with rat anti-perforin mAb AL-24 (13) (clone CE2.2, raised against recombinant mouse perforin, cross-reacting with human perforin; ascites, diluted 1:1000) and the following mouse mAbs: anti-CD2 (Becton-Dickinson, Heidelberg, Germany; diluted 1:10), anti-CD3 (Becton-Dickinson; diluted 1:10), anti-CD4 (DAKO M716, Dakopatts, Hamburg, Germany; diluted 1:10), anti-CD8 (DAKO M707; diluted 1:10) or FITC-conjugated anti-CD8 (Becton-Dickinson; diluted 1:10). The perforin-specific mAb was immunolocalized with rabbit anti–rat Ig (DAKO Z455; diluted 1:50), biotin-SP-conjugated F(ab)2 fragment donkey anti–rabbit IgG (Dianova, Hamburg, Germany; diluted 1:50) and rhodamine-labelled streptavidin (Dianova; diluted 1:100). The other mAbs were visualized using FITC-conjugated goat anti-mouse IgG (DAKO F261; 1:50). Normal rat serum and isotype-matched mouse control IgG were substituted for primary antibodies in negative control experiments.

Confocal laser microscopy. Immunostained sections were examined with a Zeiss LSM laser confocal system mounted on a Zeiss Axiovert 135M microscope equipped with the appropriate filters. Rhodamine was excited with the 543 nm line of the Argon-Krypton laser.

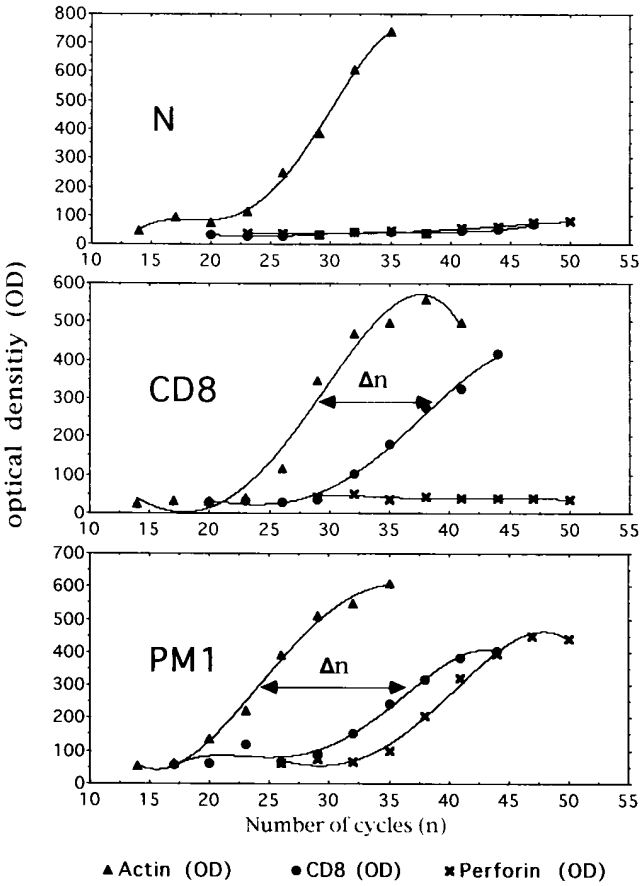

Figure 1. Comparative kinetic analysis of PCR product yields for β-actin (▲), CD8 (●), and perforin (×). The representative curves show the relationship between the amount of PCR product as measured by densitometry (OD, ordinate) and the number of amplification cycles (N, abscissa). The difference in the number of amplification cycles, denoted Δn, provides a semiquantitative measure of mRNA (15). *N*, normal muscle; *CD8*, CD8+ T cells from peripheral blood; *PM1*, polymyositis muscle (case 1).

Table I. Semiquantitative Determination of Perforin and CD8 mRNA in Muscle Biopsy Specimens

Biopsy	Δn (CD8)	Δn (perforin)
PM1	12	16
PM2	14	16
PM3	17	19
PM4	15	22
DM1	13	20
DM2	18	23
DM3	19	17
DM4	22	22
N1	>30	>30
N2	>30	>30
N3	>30	>30
N4	27	27
TE671	>30	>30
MBL	>30	>30
CD8	9	>30
LAK	11	8

The relative amounts of CD8 and perforin mRNA in muscle biopsy specimens (N, normal or neurogenic control muscle) and cell lines (TE671, human rhabdomyosarcoma; MBL, normal human myoblasts; CD8, CD8+ human T cells from peripheral blood; *LAK*, lymphokine activated killer cells) has been estimated from the difference in the number of PCR cycles (Δn) required to reach identical product levels (see also Fig. 1).

Optical sections were made in the XY plane and images were acquired by standard methods. Grey scales were converted to color images.

RNA extraction and cDNA synthesis. Total RNA was extracted from frozen muscle or cell preparations with the guanidinium thiocyanate method (14). Single-stranded cDNA was synthesized from 5 μg/ml of total RNA using oligo(dT) (Pharmacia, Freiburg, Germany) and reverse transcriptase (SuperScript™, GIBCO BRL, Eggenstein, Germany).

Semiquantitative PCR. For all PCR experiments, single-stranded cDNA was used as a template. The following primer pairs were used for amplification in separate reactions: Human perforin (Genbank/EMBL HSPRF1A): forward primer DJ10 5′-ATGTAACCAGGGCCAAAGTCA-3′ (position 3587 of the genomic sequence), backward primer DJ29 5′-GGGGTTCCAGGGTGTAGTCC-3′ (position 5492); human β-actin (Genbank/EMBL HSAC07): forward primer DJ18 5′-GGCATCGTGATGGACTCCG-3′ (position 489), backward primer DJ19 5′-GCTGGAAGGTGGACAGCGA-3′ (position 1083); human CD8: 5′-TTTCGGCGAGATACGTCTAACCCTGTGC-3′ and 5′-TTTAGCCTCCCCCTTTGTAAAACGGGCG-3′, spanning a 379-bp fragment (Clontech, ITC Biotechnology, Heidelberg, Germany).

Reactions for each primer were carried out in a total volume of 50 μl containing 1 U *Taq* polymerase (Perkin-Elmer, Applied Biosystems, Weiterstadt, Germany), 200 μM of each deoxynucleotide, 40 pmol of each primer in buffer supplied by the manufacturer. Hot start PCR was done using master mixes providing equal cDNA and *Taq*-polymerase concentrations. Individual cycles consisted of 1 min denaturation at 93°C, 1 min annealing at 60°C and 1 min extension at 72°C. Quantification was done according to Kinoshita et al. (15) with the following modifications. Aliquots were taken from the reaction mixture every 3 cycles starting after cycle 14 (β-actin), cycle 23 (perforin)

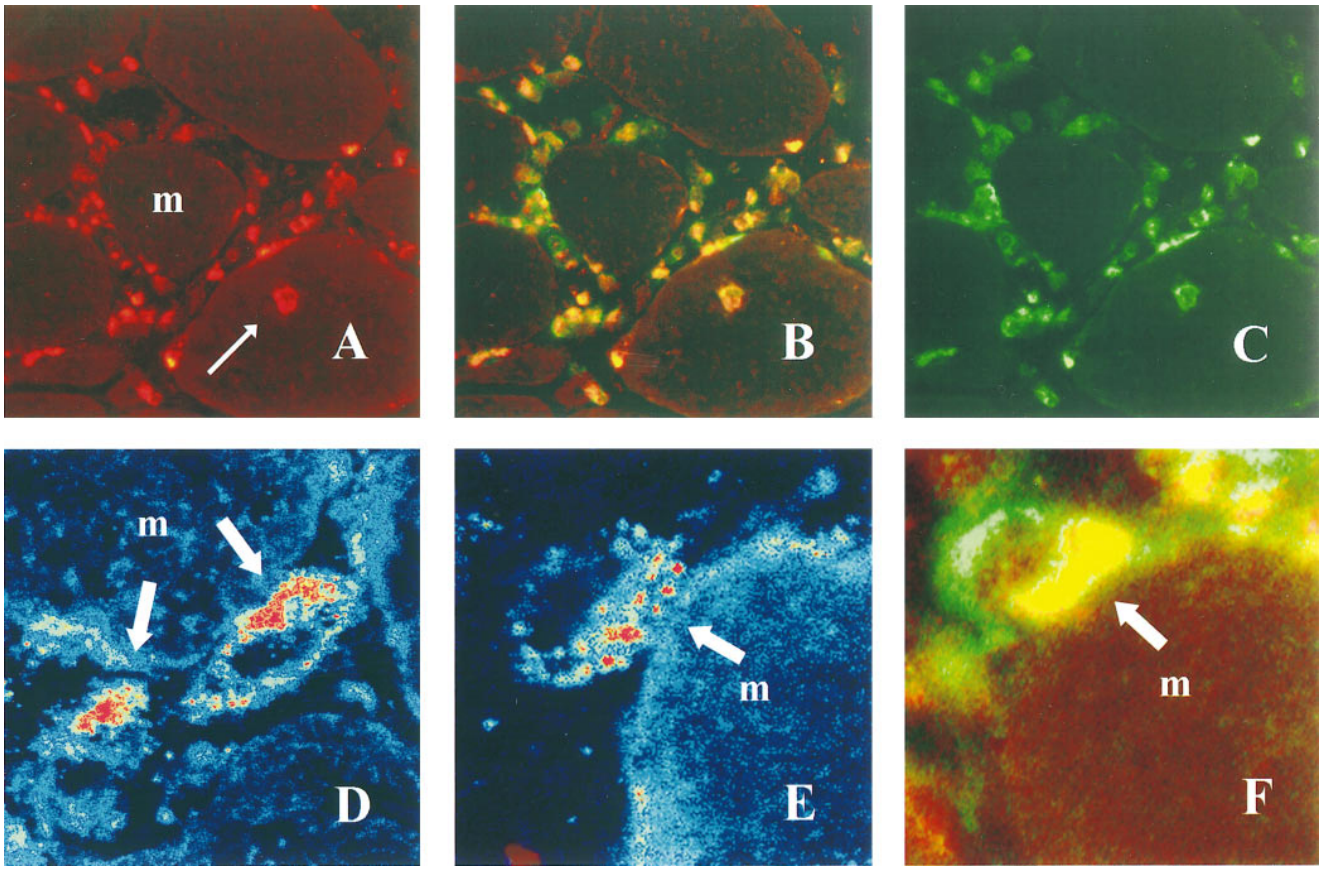

Figure 2. Immunohistochemical analysis of perforin-expressing cells in PM. (*A–C*) Colocalization of perforin (*A*; red, rhodamine) and CD3 (*C*; green, FITC) in T cells that surround and invade muscle fibers (*m*). *B* represents a double-exposure. Note the autoinvasive CD3+perforin+ T cell that has deeply penetrated into a muscle fiber (*thin arrow* in *A*). ×360. (*D–E*) confocal laser microscopical localization of perforin (red) in T cells contacting a muscle fiber (m). Note vectorial orientation of perforin towards the area of contact (*large arrows*). ×2140. (*F*) colocalization of perforin (red, rhodamine) and CD8 (green, FITC) in a T cell by double-fluorescence (conventional) microscopy. Perforin, which is oriented towards the muscle fiber (*m*), appears yellow due to overlap of the red and green signal. ×2140.

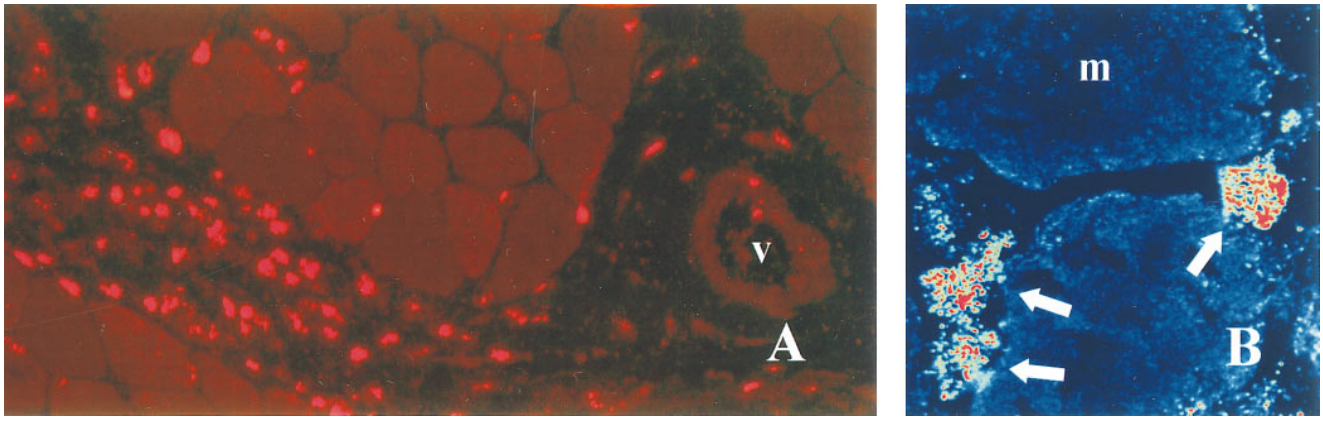

Figure 3. Immunohistochemical analysis of perforin-expressing cells in DM. (*A*) localization of perforin (red, rhodamine) in perivascular and perimysial inflammatory cells. V indicates blood vessel. ×360. (*B*) confocal laser microscopical demonstration of perforin in T cells (*arrows*) located in close proximity of muscle fibers in DM. Perforin is distributed randomly in the cytoplasm of the T cells. ×1100.

or cycle 20 (CD8), and electrophoresed in 1% agarose gels under standardized conditions. After staining with ethidium bromide, UV-induced fluorescence of specific bands was quantified in correlation to a DNA mass standard (GIBCO BRL, Eggenstein, Germany) using a video-based digitizer (Vilber Lourmat Bio1D/V6.02c, Marne La-Vallee, France). Relative OD values were graphically evaluated as shown in Fig. 1. As demonstrated by Kinoshita et al. (15), the difference in the number of cycles (Δn) needed to reach identical yields of

the PCR products as compared to the internal β-actin standard in the exponential range of amplification correlates well with the relative amount of specific mRNA in the initial sample.

Results

Semiquantitative PCR (Fig. 1, Table I) indicates that similar levels of CD8 and perforin are expressed in PM and DM but not in control muscle. Table I compares the differences in the number of PCR cycles (Δn) between the CD8 or perforin reactions and the number of cycles required for amplification of similar levels of cDNA coding for β-actin. In PM, Δn(CD8) ranged between 12 and 17, and Δn(perforin) between 16 and 22. In DM, Δn(CD8) ranged between 13 and 22, and Δn(perforin between 17 and 23. In contrast, in 3 of 4 normal muscle specimens, in normal myoblasts, and in the muscle cell line TE671 (i.e., tissue and cells not expected to express CD8 or perforin), CD8 and perforin were not detectable (Δn[CD8] and Δn[perforin] $>$ 30; Table I). As additional controls, we analyzed the expression of perforin and CD8 in resting CD8+ T cells from a healthy donor and in LAK cells. Freshly isolated CD8+ T cells from peripheral blood expressed CD8 (Δn = 9) but not perforin (Δn $>$ 30), whereas PHA-stimulated LAK cells expressed both CD8 and perforin (Δn[CD8] = 11, Δn[perforin] = 8; Table I) at considerably higher levels than myositis muscle.

Next, we investigated the expression of perforin at the protein level, using double immunofluorescence labelling for the co-localization of perforin with CD8, CD4, CD3 or CD2. The general distribution of inflammatory cells was similar to that reported in previous studies (16, 17), i.e., predominantly endomysial in PM and predominantly perivascular and perimysial in DM (Figs. 2 *A* and 3 *A*). The overall CD4/CD8 ratio was 1.1 in PM and 1.2 in DM. The total number of CD8+ inflammatory cells in 9 randomly chosen high power microscopic fields was 236 in PM and 167 in DM. Thus, substantial numbers of CD8+ T cells were present both in PM and DM muscle, consistent with the PCR results (Table I).

In agreement with the PCR results, perforin was not detected in control muscle. However, in all cases of PM and DM analyzed, the inflammatory infiltrates contained abundant perforin-expressing cells (Figs. 2 *A* and 3 *A*). The topographical distribution of the perforin+ cells was similar to the general distribution of inflammatory cells (Figs. 2 *A* and 3 *A*). In both diseases and in all cases studied, more than 90% of the perforin+ cells were CD2+CD3+. In PM, perforin was expressed both in noninvasive interstitial T cells and in autoinvasive CD8+ T cells (Fig. 2, *A–C*). Of all perforin+ cells, $\sim$ 60% were CD8+ and $\sim$ 40% CD4+. Conversely, $\sim$ 75% of the CD8+ cells and 50% of the CD4+ cells were perforin+. In DM, $\sim$ 50% of all perforin+ cells were CD4+ and 50% were CD8+. Conversely, 80% of the CD4+ cells and 90% of the CD8+ cells were perforin+.

Although the overall expression of perforin was similar in DM and PM, there was a striking difference in the intracellular distribution of perforin. Using confocal laser microscopy and high-resolution double-fluorescence immunohistochemistry, we found in PM that 43% (77/176 cells; five cases analyzed) of the T cells that contacted a muscle fiber (but none of 139 T cells that did not contact a fiber) oriented their perforin towards the contact area (Fig. 2, *D–F*). In contrast, in DM no vectorial distribution of perforin was seen in 73 of 75 T cells (97%; 4 cases; $P < 0.005$) located in close proximity to a muscle fiber (Fig. 3 *B*).

Discussion

Using PCR and immunohistochemistry, we demonstrate that perforin is expressed in muscle-infiltrating T cells both in PM and DM. However, there is a striking difference in the intracellular location of perforin, as revealed by confocal laser microscopy. In PM—but not in DM—almost half of the T cells that contact a muscle fiber orient perforin towards the contact area.

As is known from previous studies (16–18), the autoaggressive T cells that contact and invade nonnecrotic muscle fibers in PM represent activated CD3+CD8+ T cells. However, both in DM and PM, about 50% of the perivascular and perimysial T cells and also 20% of the (noninvasive) endomysial T cells are CD4+ (16). The cells that stained positive with the anti-perforin mAb AL-24 included both CD8+ and CD4+ cells. There is no indication that the mAb AL-24 reacts to other granule-associated molecules, although it is difficult to positively rule out this possibility. The observation that a substantial proportion of CD4+ inflammatory T cells express perforin in situ is not unprecedented, since CD4+perforin+ T cells were also detected in thyroid tissue in Hashimoto's thyroiditis with a different mAb (19). Furthermore, it has been demonstrated that perforin can be induced in CD4+ T cells in vitro (1–6, 20).

The redistribution of perforin in autoinvasive CD8+ T cells towards the membrane of the target muscle fiber clearly indicates the important pathogenic potential of perforin in PM as compared to DM. Because the vectorial secretion of cytotoxic granules in a TCR-dependent step (6, 21–24), our results provide morphological evidence that in PM the CD8+ T cells recognize an unknown antigen on the muscle fiber surface. It has been well established that conjugation of the cytotoxic with the target cell transmits signals to the killer cell to position its secretory apparatus, microtubule organizing center, Golgi complex, and cytolytic granules towards the contact site (6, 21, 22). After conjugation and reorientation, individual granules are secreted in the direction of the target cell. Granule exocytosis results in the release of cytotoxic molecules, perforin and proteases (granzymes) (1–6).

In the early stages of muscle fiber invasion, the surface membrane of muscle fibers appears to remain intact at the light microscopic (17) and electronmicroscopic (18) level. Pore-like structures could not be detected in the sarcolemma of muscle fibers attacked by T cells in PM (18). One possible explanation is that perforin pores/channels on nucleated cells in vivo are smaller in size than the pores generated in vitro on erythrocytes and other target cells by the addition of purified perforin. Perforin pores containing less than 10–20 monomers would escape detection by electron microscopy (5). Another explanation for the lack of morphologically visible muscle cell damage is that the surface membrane of the muscle fiber is rapidly repaired at least during the early stages of muscle fiber invasion. Repair could occur, for example, by shedding or endocytosis of pore-damaged membrane (reviewed in reference 3).

As pointed out by Arahata and Engel (18), it is interesting to note in this connection that the volume of a 25-mm-long and 50-μm-wide muscle fiber is nearly 28,000-fold larger than, for example, that of a spherical 15-μm tumor cell. Perforin pores, which electrophysiologically behave like nonselective ion

channels (25), would allow the influx of calcium. Consistent with this assumption is the observation that invaded muscle fibers show signs of focal myofibrillar degeneration near invading cells (18). These changes could be a consequence of membrane insertion of perforin and focal protease activation (18). Another indirect sign of muscle fiber damage is the intense focal regenerative activity noted in areas immediately adjacent to autoinvasive T cells (18).

Previous immunohistochemical data on perforin expression in inflammatory myopathies differ from our results (26). Using a mAb raised against an amino-terminal synthetic peptide of perforin, the authors observed faint immunoreactivity in about 10% of endomysial CD8+ T cells in PM, but found only very few immunoreactive T cells in DM (26). In contrast, our immunohistochemical data were obtained with a mAb raised against recombinant perforin and were corroborated by PCR, confirming perforin expression both in PM and DM. Thus, we conclude that our mAb is more sensitive and suitable for immunohistochemical analyses than the anti-peptide mAb (26).

Our observation that perforin is expressed both in DM and PM is supported by PCR analysis of granzyme B, which we also found expressed in DM and PM (not shown). That perforin is expressed both in CD4+ and CD8+ T cells, and in invasive and noninvasive T cells indicates that total perforin expression (as measured by semiquantitative PCR) reflects polyclonal T cell activation rather than the number of Ag-specific autoaggressive T cells. Consistent with this interpretation, and exemplified by our PCR analysis of freshly isolated CD8+ T cells, resting circulating T cells do not express perforin constitutively (5, 20). Both CD4+ and CD8+ T cells can, however, be induced to express perforin by various cytokines and mediators, such as interleukin-2 (20, 27). In the inflammatory muscle lesions of PM and DM, the T cells are most likely stimulated by high local concentrations of cytokines secreted by inflammatory T cells and macrophages. Consistent with this view, a recent PCR study of the expression in muscle of interleukins-1, -2, -4, -5, -6, interferon-γ, tumor necrosis factor-α, granulocyte-macrophage colony stimulating factor and transforming growth factors β1 and β2 reported no substantial difference in cytokine expression between PM and DM, except that interleukin-4 was expressed moderately to strongly only in PM but not DM (28).

As pointed out in earlier reports of perforin expression in autoimmune disease and transplant rejection (29–33), the demonstration of perforin by PCR and/or immunohistochemical methods does not necessarily imply a direct role in tissue injury. PM, however, has the unique advantage that the autoaggressive (autoinvasive) T cells can be distinguished morphologically (7–9, 17). The autoinvasive CD8+ T cells are clonally expanded and express a highly restricted TCR repertoire (10). Because TCR stimulation is known to induce the polarized secretion of perforin towards the target cell membrane (6, 23, 24), the polarized intracellular orientation of perforin in the CD8+ T cells that contact or invade muscle fibers strongly suggests that these T cells recognize an as yet unidentified (auto-)antigen via their TCR on the muscle fiber surface.

Acknowledgments

We thank Drs. Richard Albrecht and John Murphy for their help with confocal microscopy; Dr. Andrew G. Engel for his helpful comments on the manuscript; Ms. Martina Sölch and Sybille Galuschka for excellent technical assistance; and Dr. Jim Chalcroft for his help with the figures.

This work was supported by the Deutsche Forschungsgemeinschaft (SFB 217, C13) and Wilhelm Sander-Stiftung.

References

1. Tschopp, J., and M. Nabholz. 1990. Perforin-mediated target cell lysis by cytolytic T lymphocytes. *Annu. Rev. Immunol.* 8:279–302.

2. Podack, E.R., H. Hengartner, and M.G. Lichtenheld. 1991. A central role of perforin in cytolysis? *Annu. Rev. Immunol.* 9:129–148.

3. Henkart, P.A. 1994. Lymphocyte-mediated cytotoxicity: two pathways and multiple effector molecules. *Immunity*. 1:343–346.

4. Berke, G. 1994. The binding and lysis of target cells by cytotoxic lymphocytes: Molecular and cellular aspects. *Annu. Rev. Immunol.* 12:735–773.

5. Liu, C.-C., C.M. Walsh, and J.D.-E. Young. 1995. Perforin: Structure and function. *Immunol. Today.* 16:194–201.

6. Henkart, P.A., M.S. Williams, and H. Nakajima. 1995. Degranulating cytotoxic lymphocytes inflict multiple damage pathways on target cells. *Curr. Top. Microbiol. Immunol.* 198:75–93.

7. Hohlfeld, R., and A.G. Engel. 1994. The immunobiology of muscle. *Immunol. Today.* 15:269–274.

8. Engel, A.G., R. Hohlfeld, and B.Q. Banker. 1994. The polymyositis and dermatomyositis syndromes. *In* Myology. A.G. Engel and C. Franzini-Armstrong, editors. McGraw Hill, New York. 1335–1383.

9. Dalakas, M.C. 1991. Polymyositis, dermatomyositis and inclusion-body myositis. *N. Engl. J. Med.* 325:1487–1498.

10. Bender, A., N. Ernst, A. Iglesias, K. Dornmair, H. Wekerle, and R. Hohlfeld. 1995. T cell receptor repertoire in polymyositis: Clonal expansion of autoaggressive CD8+ T cells. *J. Exp. Med.* 181:1863–1868.

11. Emslie-Smith, A.M., and A.G. Engel. 1990. Microvascular changes in early and advanced dermatomyositis: A quantitative study. *Ann. Neurol.* 27: 343–356.

12. Goebels, N., D. Michaelis, H. Wekerle, and R. Hohlfeld. 1992. Human myoblasts as antigen presenting cells. *J. Immunol.* 149:661–667.

13. Dupuis, M., E. Schaerer, K.-H. Krause, and J. Tschopp. 1993. The calcium-binding protein calreticulin is a major constituent of lytic granules in cytolytic T lymphocytes. *J. Exp. Med.* 177:1–7.

14. Chomczynski, P., and N. Sacchi. 1987. Single-step method of RNA isolation by acid guanidium thiocyanate-phenol-chloroform extraction. *Anal. Biochem.* 162:156–159.

15. Kinoshita, T., T. Imamura, H. Nagai, and K. Shimotohno. 1992. Quantification of gene expression over a wide range by the polymerase chain reaction. *Anal. Biochem.* 205:231–235.

16. Arahata, K., and A.G. Engel. 1984. Monoclonal antibody analysis of mononuclear cells in myopathies. I. Quantitation of subsets according to diagnosis and sites of accumulation and demonstration and counts of muscle fibers invaded by T cells. *Ann. Neurol.* 16:193–208.

17. Engel, A.G., and K. Arahata. 1984. Monoclonal antibody analysis of mononuclear cells in myopathies. II. Phenotypes of autoinvasive cells in polymyositis and inclusion body myositis. *Ann. Neurol.* 16:209–216.

18. Arahata, K., and A.G. Engel. 1986. Monoclonal antibody analysis of mononuclear cells in myopathies. III. Immunoelectron microscopy aspects of cell-mediated muscle fiber injury. *Ann. Neurol.* 19:112–125.

19. Wu, Z., E.R. Podack, J.M. McKenzie, K.J. Olsen, and M. Zakarija. 1994. Perforin expression by thyroid-infiltrating T cells in autoimmune thyroid disorders. *Clin. Exp. Immunol.* 98:470–477.

20. Liu, C.-C., S. Rafii, A. Granelli-Piperno, J.A. Trapani, and J.D.-E. Young. 1989. Perforin and serine esterase gene expression in stimulated human T cells. Kinetics, mitogen requirements, and effects of cyclosporin A. *J. Exp. Med.* 170:2105–2118.

21. Kupfer, A., and S.J. Singer. 1989. Cell biology of cytotoxic and helper T-cell functions. *Annu. Rev. Immunol.* 7:309–338.

22. Podack, E.R., and A. Kupfer. 1991. T cell effector mechanisms for delivery of cytotoxicity and help. *Annu. Rev. Cell Biol.* 7:479–504.

23. Yannelli, J.R., J.A. Sullivan, G.L. Mandell, and V.H. Engelhard. 1986. Reorientation and fusion of cytotoxic granules after interaction with target cells as determined by high resolution cinematography. *J. Immunol.* 136:377–382.

24. Kupfer, A., S.J. Singer, and G. Dennert. 1986. On the mechanism of unidirectional killing in mixtures of two cytotoxic T lymphocytes. Unidirectional polarization of cytoplasmic organelles and the cytoskeleton in the effector cell. *J. Exp. Med.* 163:489–498.

25. Felzen, G., G. Berke, D. Rosen, R. Coleman, J. Tschopp, J.D.-E. Young, and O. Binah. 1994. Effects of purified perforin and granzyme A from cytotoxic T lymphocytes on guinea pig ventricular myocytes. *Cardiovascul. Res.* 28: 643–649.

26. Orimo, S., R. Koga, K. Nakamura, M. Arai, M. Tamaki, H. Sugita, I. Nanaka, and K. Arahata. 1994. Immunohistochemical analysis of perforin and granzyme A in inflammatory myopathies. *Neuromusc. Disord*. 4:219–226.

27. Smyth, M.J., J.R. Ortaldo, Y.-I. Shinkai, H. Yagita, M. Nakata, K. Oku-

mura, and H.A. Young. 1990. Interleukin 2 induction of pore-forming protein gene expression in human peripheral blood CD8+ T cells. *J. Exp. Med.* 171: 1269–1282.

28. Lundberg, I., J.M. Brengman, and A.G. Engel. 1995. Analysis of cytokine expression in muscle in inflammatory myopathies, Duchenne dystrophy and non-weak controls. *J. Neuroimmunol.* 63:9–16.

29. Young, L.H.Y., S.V. Joag, L.-M. Zheng, C.-P. Lee, and J.D.-E. Young. 1990. Perforin-mediated myocardial damage in acute myocarditis. *Lancet.* 336:1019–1021.

30. Hameed, A., K.J. Olsen, L. Cheng, W.M. Fox, R.H. Hruban, and E.R. Podack. 1992. Immunohistochemical identification of cytotoxic lymphocytes using human perforin monoclonal antibody. *Am. J. Pathol.* 140:1025–1030.

31. Griffiths, G.M., R. Namikawa, C. Mueller, C.-C. Liu, J.D.-E. Young, M. Billingham, and I. Weissman. 1991. Granzyme A and perforin as markers for rejection in heart transplantation. *Eur. J. Immunol.* 21:687–693.

32. Legros-Maïda, S., A. Soulié, C. Benvenuti, A. Wargnier, N. Vallée, C. Berthou, J. Guillet, M. Sasportes, and N. Sigaux. 1994. Granzyme B and perforin can be used as predictive markers of acute rejection in heart transplantation. *Eur. J. Immunol.* 24:229–233.

33. Lipman, M.L., A.C. Stevens, and T.B. Strom. 1994. Heightened intragraft CTL gene expression in acutely rejecting renal allografts. *J. Immunol.* 152: 5120–5127.